Journal of Molecular Catalysis, *25* (1984) 193 - 206

ADSORPTION AND DECOMPOSITION OF CO ON Cu, Ni AND Cu—Ni SINGLE CRYSTALS

O. L. J. GIJZEMAN, C. M. A. M. MESTERS, F. LABOHM and J. W. GEUS

Van 't Hoff Laboratory, University of Utrecht, Padualaan 8, 3584 CH Utrecht (The Netherlands)

Summary

The adsorption of CO on Ni(100), Ni(111) and Cu—Ni surface alloys has been studied in the temperature range 300 - 600 K and pressures up to 10^{-2} torr. Adsorption isotherms on pure nickel gave a coverage-independent heat of adsorption of 134 kJ mol^{-1}. If, on Ni(111), some carbon was present on the surface this value decreased to 103 kJ mol^{-1}. On Cu—Ni surface alloys no CO adsorption was found for Cu(100)—Ni, and on Cu(111)—Ni adsorption-induced segregation was so severe that no heat of adsorption could be determined. For low nickel content on Cu(110)—Ni the heat of adsorption is 62 kJ mol^{-1}; at higher nickel fractions this value increases to 75 kJ mol^{-1}, with a small amount of CO bound with 75 - 130 kJ mol^{-1}. At very high nickel concentration, segregation of Ni made accurate determinations impossible. On Ni(100) and Ni(111), CO disproportionates, but more readily on Ni(100). On Cu—Ni surface alloys no carbon deposition took place. These results are compared with literature data and an explanation for the difference between Cu and Ni in the CO disproportionation reaction is given. The differences and similarities between the three low-index faces are also discussed.

Introduction

In this paper we discuss the adsorption and decomposition of carbon monoxide on the low-index faces of copper, nickel and copper–nickel alloys. The importance of these systems for catalysis need not be stressed again here. Rather, we will outline in this section the merits and demerits of the techniques used to study these systems under ultra-high vacuum conditions for those readers unfamiliar with them.

The most widely used technique in surface science is undoubtedly Auger Electron Spectroscopy (AES) [1 - 3]. This method provides a qualitative analysis for all elements (except hydrogen and helium) and in most cases, after calibration, a semi-quantitative analysis. In this paper Auger peak

0304-5102/84/$3.00

heights, measured in the derivative mode [1], are denoted as h, a larger value of h corresponding to a higher surface coverage. Due to the inelastic scattering of Auger electrons, only those originating from the near-surface region (3 - 15 Å) contribute to the signal. This information depth depends on the kinetic energy of the Auger electrons and thus on the particular Auger peak monitored in the spectrum. This effect is exploited in our study on Cu—Ni alloys where the intensity of the Ni(101 eV) and Ni(720 eV) or Ni(848 eV) transitions gives information on the amount of nickel in the first two and the topmost 6 - 8 layers respectively. A disadvantage of AES is, of course, that the electron beam may cause dissociation and/or desorption of adsorbates. This is particularly cumbersome for CO, a widely studied adsorbate.

In our work on CO adsorption we have used ellipsometry to monitor the CO surface coverage. Basically, an ellipsometer measures the change in polarisation of a monochromatic light beam upon reflection from a bare and adsorbate-covered surface [4, 5]. Since for most systems the reflection coefficient of the light is near unity, no energy is transferred to the system studied and its disturbance is minimal.

The ellipsometric parameters used in this paper are $\delta\Delta$ and $\delta\psi$. They refer to angular settings of polarisers and are expressed in degrees. In the simplest approximation both should be proportional to (sub)monolayer coverages [6, 7], but exceptions occur. In the case of CO adsorption, $\delta\Delta$ is believed to be linearly related to the CO coverage [8]. The information depth of ellipsometry is roughly the distance that the light penetrates into the substrate. For many metals this is of the order of 60 - 300 Å, so subsurface concentrations of foreign atoms can also be detected, well outside the range accessible to AES. The disadvantage of ellipsometry is its *a priori* unknown dependence of $\delta\Delta$ and $\delta\psi$ on coverage and its non-specificity to different elements. Nevertheless, a combination of this technique with AES (and other surface-sensitive methods) has revealed many features of the adsorption of CO and the kinetics of the CO oxidation on oxygen-covered Cu, Ni and Cu—Ni surfaces [7].

In the next sections we will discuss the adsorption of CO on copper, nickel and copper–nickel alloys as measured by us and many other authors. For details of experimental procedures the reader is referred to the original papers. In general all surfaces investigated were clean, annealed, crystal faces of the appropriate orientation.

Adsorption of CO on copper single cyrstals

Significant adsorption of CO on copper single crystals is only found at low temperatures ($T < 300$ K). In all cases reported no dissociation of adsorbed CO occurs. Notably Pritchard and coworkers have studied these systems using work function measurements, low energy electron diffraction (LEED) and infrared spectroscopy to determine the adsorption states

(bridge-bonded *versus* linearly bound), overlayer structures, and heats of adsorption [9]. For future reference some of their results are collected in Table 1.

In our own work, using ellipsometry, we have likewise been unable to detect any CO adsorption on clean low-index copper surfaces at room temperature and pressures up to 10^{-3} torr. It should be noted that also on oxygen-covered surfaces, on which CO is readily oxidised [7], the presence of CO cannot be established. Electron beam induced decomposition of CO on Cu seems less of a problem than on Ni surfaces. In fact, even sputtering a clean Cu(111) surface with CO (5×10^{-5} torr, 500 eV) does not lead to a detectable amount of carbon on the surface, as verified by AES.

Adsorption of CO on nickel single crystals

In contrast to copper, nickel surfaces do adsorb CO at room temperature and above. At room temperature the adsorption is non-dissociative, but some evidence for dissociation at steps has been reported [20]. At higher temperatures ($T > 420$ K) CO decomposes on Ni(100), leaving the surface covered with mainly carbon and virtually no oxygen [17]. The presence of this carbon inhibits the adsorption of CO. Depending on the CO pressure during decomposition, CO adsorption is completely suppressed for carbon coverages of 0.25 to 0.5 monolayers (see Fig. 1). The CO coverage was determined by a linear interpolation of the measured $\delta\Delta$ values between zero ($\theta_{CO} = 0$) and the observed saturation value, where $\theta_{CO} = 0.69$. The carbon coverage was determined by AES, using the known peak height corresponding to $\theta_C = 0.5$ from the decomposition of ethylene on Ni(100) [17]. A similar observation has been made with respect to carbon deposited on Ni(100) by the electron-induced disproportionation of CO [8].

Adsorption isotherms of CO on clean Ni(111) and Ni(100) are shown in Fig. 2. These were determined using ellipsometry and show $\delta\Delta$, which is proportional to surface coverage, *versus* $\ln P$. The accessible temperature range is restricted to $T < 420$ K for Ni(100) due to CO disproportionation [17] and to $T < 530$ K for Ni(111), being limited only by the low coverages obtained at higher temperatures. The slope of a plot of $\ln P$ at constant coverage (*i.e.* at constant $\delta\Delta$) *versus* $1/T$ gives the isosteric heat of adsorption. These are given in Table 1 and compared to literature values, where the agreement is seen to be very good. The shape of the isotherms can be quantitatively explained by assuming an infinite repulsion between two CO molecules adsorbed on nearest-neighbour sites [15, 17]. This repulsion is caused by the CO molecules themselves, and not so much influenced by the underlying substrate. The intermolecular potential for two parallel gas phase CO molecules can be computed with *ab initio* techniques and is shown in Fig. 3 [15]. It is seen that in this configuration the interaction energy is zero at a distance of about 3.3 Å. For a hexagonal close-packed array of hard cylinders, this results in a coverage of 1×10^{15} molecules cm^{-2}, in good

TABLE 1

Properties of Cu, Ni and Cu—Ni alloys. Given are the number of sites (N_s) and the maximum CO coverage (N_{max}); the heat of adsorption and experimental conditions are also listed

	Cu					Cu—Ni			Ni					
	(111)			(100)	(110)		(111)	(100)	(110)	(111)		(100)	(110)	
N_s (10^{15} cm^{-2})	1.77			1.53	1.08		(1.82)	(1.57)	(1.11)	1.86		1.61	1.14	
N_{max} 10^{15} cm^{-2})	0.92			0.89	0.86		—	—	(1.11)	1.06	0.99	1.17	1.14	
reference	[9, 10]			[10]	[11]		[a]	[12]	[13, a]	[14, 15]	[16]	[17, 18]	[19]	
ΔH (kJ mol^{-1})	50	38		54.6	55	55 → 30	[a]	not ads.	130 → 75	134	111	134 128	125	104
θ	0 → 1/3	1/3 → 0.52			0 → 0.5	0.5 → 0.8	[a]		0 → ~1	0 → 0.54		0 → 0.7	0 → 0.6	0.7 → 1
T (K)	77 - 200			—	> 77		[a]	293	350 - 460	390 - 530		370 - 420	310 - 500	

[a] This work.

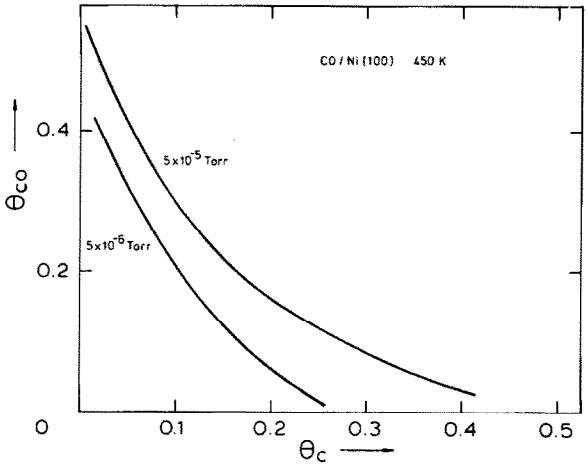

Fig. 1. Amount of carbon monoxide adsorbed (θ_{CO}) as a function of the amount of carbon on Ni(100) during the disproportionation of CO at two different pressures.

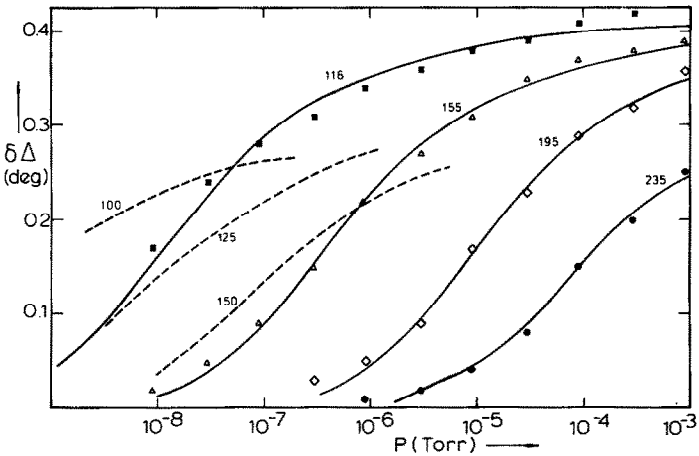

Fig. 2. Adsorption isotherms of CO on Ni(100) (— — —) and Ni(111) (———). Temperatures are indicated in °C. The vertical axis is proportional to the CO coverage, but the proportionality constant is different for the two crystal faces, as the saturation coverage is the same.

agreement with the saturation values obtained experimentally (*cf.* Table 1).

This picture changes drastically when the Ni surface is contaminated with carbon. Figure 4 shows the adsorption isotherms of CO on Ni(111) on which about 1/3 to 1/2 monolayer of carbon had been deposited by the thermal decomposition of ethylene. Decomposition took place at a crystal temperature of 250 °C and ethylene pressures of 10^{-7} torr. The surface carbon coverage was estimated via AES by comparison with Ni(100)/C. It was found [21] that some carbon is also taken up below the surface, so that the

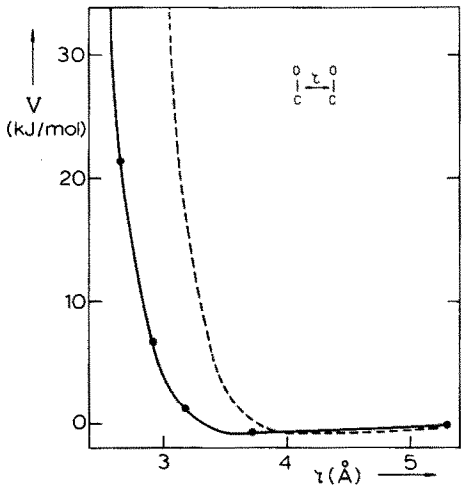

Fig. 3. Interaction energy of two parallel CO molecules as a function of their distance (——). For comparison, the Lennard–Jones potential for randomly oriented molecules is indicated (- - -).

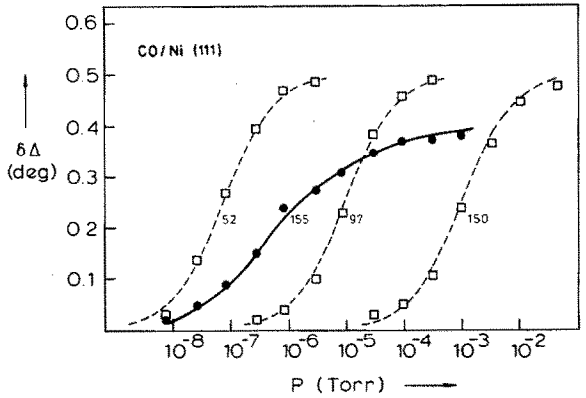

Fig. 4. Adsorption isotherms of CO on Ni(111) with 0.3 - 0.5 monolayer of carbon, deposited from ethylene, on the surface. For comparison, one isotherm on the clean surface is included. Temperatures are indicated in °C. The dashed lines are Langmuir isotherm fits to the data points.

crystal must be somewhat rough or disordered, as evidenced by the absence of a LEED pattern. The isotherms are seen to shift to higher pressures (for equal temperature) and to change shape as well. The isosteric heat of adsorption now drops to 103 kJ mol^{-1}, again independent of coverage. Surprisingly, these isotherms obey the simple Langmuir equation in all cases [21]. Since the saturation value of $\delta\Delta_{CO} \simeq 0.5°$ is higher on the carbon-covered surface (see Fig. 4), this surface must adsorb more CO than the clean Ni surface, if the changes in Δ due to carbon and CO are additive. This is true on theoretical grounds, but more convincingly demonstrated by the fact

that the saturation value of $\delta\Delta_{CO}$ was found to be 0.5° for both a nickel surface that contained an amount of carbon that changed the value of the clean surface by $\delta\Delta_C = 0.2°$, and a surface with $\delta\Delta_C = 0.4°$. For the two cases the surface carbon coverage as measured by AES was the same, so that one expects the same maximum CO uptake. The presence of subsurface carbon thus causes a roughening of the surface, leading to a higher site density for CO adsorption.

These results seem to be at variance with those obtained for CO adsorbed on Ni(100)/C described earlier in this section, where it was stated that carbon obtained from CO lowered the capability of the surface to bind CO. The difference, we believe, is explained by the nature of the carbon deposit. C obtained from CO does not behave as does C obtained from C_2H_4. Evidence for this fact is presented in Fig. 5, where two isotherms are shown, one for a Ni(111) surface contaminated with carbon from ethylene (as in Fig. 4), and one where some carbon monoxide decomposition had also taken place. It is seen that the amount of CO adsorbed decreases as carbon from CO is added, whereas extra carbon from ethylene had no effect on the isotherms. Also the C 272 eV Auger peak shape is different for C from CO and C from ethylene. It is of course not surprising that the exact electronic state of adsorbed carbon influences the adsorption behaviour of CO.

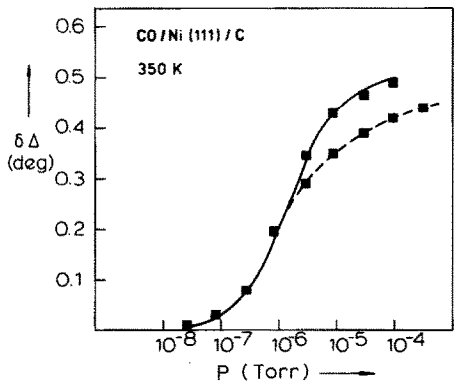

Fig. 5. Adsorption isotherms of CO on Ni(111) contaminated with carbon deposited from ethylene (——) and some additional carbon deposited from CO (— — —).

CO disproportionation takes place on Ni(100) above 420 K, and leads to at most one half of a monolayer of carbon. At Ni(111) this reaction is much slower and far less reproducible. It essentially occurs only above 440 K and pressures above 10^{-2} torr, and is always correlated with the appearance of sulfur on the surface. These experiments took long times (on the order of hours) so that sulfur segregation from the bulk may be the cause of the irreproducibility. A further major difference between the two crystal planes is that in the case of Ni(111) the amount of carbon deposited from CO at the surface as measured by AES is about 0.5 to 1.0 monolayer, whereas ellipsometrically a much larger quantity of carbon is detected. The differences

in information depth of the two techniques thus enable us to draw the conclusion that on Ni(111) carbon is able to penetrate the surface and to accumulate in deeper layers. Similar conclusions have also been obtained for carbon deposited from ethylene on Ni(111) [21]. The effect of sulfur has been reported to decrease the heat of adsorption of CO on Ni(100) [22] and Ni(111) [23]. It is not obvious, however, that this will also result in an enhanced disproportionation rate, since, as we have shown, carbon also decreases the heat of adsorption but does not lead to an increase in the disproportionation of CO.

Adsorption of CO on Cu—Ni surface alloys

Cu—Ni surface alloys can be prepared by exposing single crystals of pure copper to a nickel-carbonyl/CO mixture [12, 24]. At temperatures above 430 K the $Ni(CO)_4$ decomposes, leaving a surface that contains only Ni and no carbon or oxygen, except for very large exposures, where a thick nickel film is deposited [12]. Figure 6 shows the Auger spectrum of such a Cu(111)—Ni alloy. The Ni and Cu transitions are indicated in the figure, both before (left panel) and after exposure to pure CO at $P = 0.3$ torr at 50 °C. For all three copper surfaces studied, no change in the original surface structure was found by low energy diffraction, except for an increase in background intensity. Figure 7 shows the average mol fraction of nickel in the first two layers (x_L) and first 6 - 8 layers (x_H) as a function of carbonyl exposure and as determined by AES. In this determination, the difference in escape depths of two particular Auger transitions has been used. As can be seen, the average amount of nickel in the first few layers remains negligible

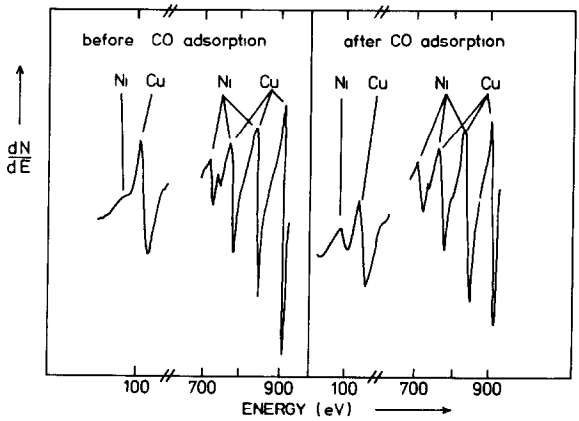

Fig. 6. Auger spectra of a Cu(111)—Ni crystal. Left spectrum: after Ni deposition up to $\delta\psi = 0.4$. The low-energy surface-sensitive Ni peak is absent. Right spectrum: after CO exposure and CO desorption. The low energy Ni peak is now visible due to induced nickel segregation.

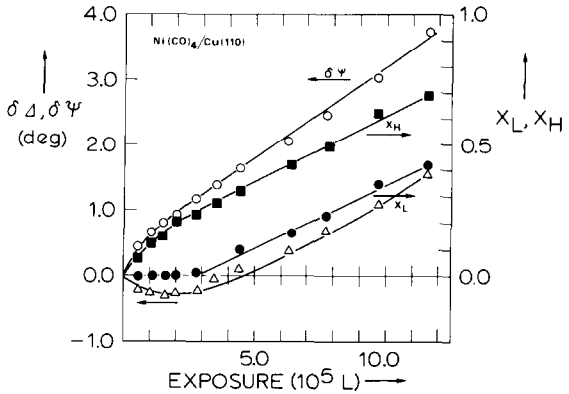

Fig. 7. Changes in the ellipsometric parameters $\delta\Delta$ (△) and $\delta\psi$ (○) as a function of $Ni(CO)_4/CO$ exposure to Cu(110). The corresponding mol fractions of Ni in the first two layers x_L (●) and the first 6 - 8 layers x_H (■) are also given.

for some time, whereas the average amount in the first 6 - 8 layers increases immediately. The inequality $x_H > x_L$ always holds. Similar observations apply to the other low-index faces. The implication is that for these systems the surface layers contain a large amount of copper, whereas the nickel is situated in deeper layers (up to 500 - 1000 layers) followed, of course, by the original clean copper crystal. Upon removing the $Ni(CO)_4/CO$ gas mixture, the nickel content of the surface did not stabilise immediately, in particular for the Cu(111)/Ni system. Since Cu—Ni form a substitutional alloy, much atomic rearrangement must occur in order to form the thermodynamically preferred structure with a copper-enriched surface. Obviously, this is less easy, starting from the close-packed (111) face.

The nickel deposition was continuously monitored with ellipsometry (*cf.* Fig. 7), using the variable $\delta\psi$ as parameter, where a larger value of $\delta\psi$ corresponds to a higher nickel content. The value of $\delta\psi$ is given in brackets after the surface alloy name in Table 2, together with the mol fractions of nickel. Carbon monoxide adsorption was studied on all alloys listed in Table 2. No CO adsorption was found at room temperature on both Cu(100)—Ni surfaces for pressures up to 10^{-3} torr. All other systems exhibited CO adsorption and thus we attempted to measure the adsorption isotherms. For coverages between 0.2 - 0.4 monolayer, the heat of adsorption on Cu(110)—Ni(0.5°) was 62 kJ mol^{-1}. The nickel-richer C(110)—Ni(1°) face showed an initial heat of adsorption of 130 kJ mol^{-1}, falling to 75 kJ mol^{-1} at a coverage of 0.14 and then maintaining this value up to $\theta \simeq 0.4$ [13]. The other two surface alloys, Cu(110)—Ni(3°) and Cu(110)—Ni(5°), were difficult to investigate accurately, due to chemisorption-induced nickel segregation during the measurement of an isotherm. A tentative value between 60 and 75 kJ mol^{-1} seems most likely. The Ni-enrichment was even more severe for Cu(111)—Ni alloys. Although the presence of CO adsorption could be established beyond doubt, the redistribution of Ni upon adsorption of CO was so great (even for low nickel content) that no adsorption

TABLE 2

Summary of Cu—Ni alloys studied. The average amount of nickel in the first two (x_L) and first 6 - 8 layers (x_H) is given, as well as the heat of adsorption and the pressure range used

	x_L	x_H	ΔH (kJ mol^{-1})	P (torr)
Cu(100)—Ni(0.7°)	0	0.25	not adsorbed	$< 10^{-3}$
—Ni(3°)	0.32	0.60	not adsorbed	$< 10^{-3}$
Cu(110)—Ni(0.5°)	0	0.11	62 $0.2 < \theta < 0.4$	10^{-7} - 1
—Ni(1°)	0	0.20	130 $\theta = 0$	10^{-7} - 1
			75 $0.15 < \theta < 0.4$	10^{-7} - 1
—Ni(3°)	0.24	0.38	60 - 75 $0.2 < \theta < 0.4$	10^{-7} - 1
—Ni(5°)	0.2 - 0.4	0.56 - 0.67	60 - 75 $0.2 < \theta < 0.4$	10^{-7} - 1
Cu(111)—Ni(0.4°)	0 - 0.1	0.15 - 0.25	adsorbed	10^{-4} - 1

isotherms could be measured. For Cu(110)—Ni(0.5°), pressures in excess of 0.05 torr and temperatures above 400 K lead to some Ni enrichment; for Cu(111)—Ni(0.4°), several exposures at 350 K and 0.4 torr lead to an increase in the nickel content of the first few layers of ~0.5 → 0.10 → 0.22 → 0.26. At 450 K this sequence was ~0.07 → 0.36 → 0.61 → 0.75, with large scatter in the data points. An example is given in Fig. 6.

The remarkable aspect of our surface alloys is their lack of CO dissociation. Only by electron bombardment or operating ionisation gauges could CO be made to disproportionate. The carbon content on Cu(110)—Ni(5°) at the surface then decreased with time, indicating that even at room temperature carbon dissolves in the bulk of the crystal. The depth profile of a clean and carbon-containing Cu(110)—Ni(5°) surface is shown in Fig. 8. If the same sputter efficiency of 3 to 4 layers per minute is assumed for both

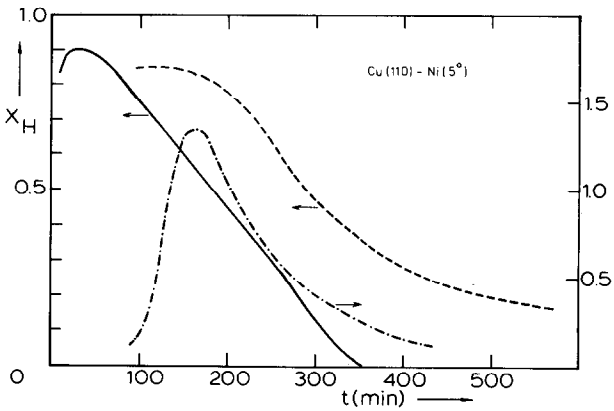

Fig. 8. Sputter profile of a clean (——) and carbon-containing Cu(110)—Ni(5°) surface alloy (— — —). The amount of carbon is seen to increase on penetrating the crystal (— · —) and to decrease again, in parallel with the amount of nickel present (— — —).

surfaces; it follows that more nickel is present in the carbon-contaminated surface, contrary to its experimental preparation. We are thus led to assume a smaller sputter efficiency for the carbon-contaminated crystals, in agreement with the natural 'hardness' of carbides. It is furthermore to be seen from Fig. 8 that the carbon profile follows that of the nickel, indicating a tendency of carbon and nickel to form some stable complex, even in a Cu matrix.

Comparisons and discussion

The first point we address in this section is the question why the capability to bind CO at room temperature decreases in the order Ni > Cu(111)—Ni, Cu(110)—Ni > Cu(100)—Ni ≃ Cu, as follows from Table 1. The two extremes, pure Cu and pure Ni, may be understood by the observation that Cu has the electronic configuration $3d^{10}4s^1$, a full d-band, whereas Ni($3d^84s^2$) has a partially filled d-band. *A priori*, one expects thus that the interaction of the doubly-occupied 5σ CO orbital will be repulsive for Cu and attractive for Ni. Contributions to back-donation from filled sub-bands will be similar for the two metals. Based on this picture, one would expect that on adding Ni to a copper crystal at or near the surface, the alloy will have a partially filled d-band as well and thus adsorb CO, although with a smaller heat of adsorption or bond strength. This is true for Cu(111)—Ni and Cu(110)—Ni, but not for Cu(100)—Ni. A possible reason for this may be found in the approach of Bond [25], Weinberg and Merrill [26] and van Santen [27]. These authors consider the spatial arrangement of the 5 d-orbitals at the crystal surface. For the (111) face, all 5 d-orbitals point away from the surface at some angle; for the (110) surface, the $d(z^2)$-orbital is parallel to the plane (all others pointing away from it at some angle), and for the (100) surface both the $d(x^2-y^2)$ and the $d(xy)$-orbitals are in the surface plane. If all orbitals are doubly occupied (as in Cu), no CO adsorption is expected in our approximation. Withdrawing electrons from them by substitutional nickel atoms, the holes created in d-orbitals parallel to the surface will not be very effective in binding CO, due to such binding being necessarily in close proximity to the surface. This leaves five potential binding orbitals for the (111) face, four for the (110) face and only three for the (100) face. Of course the occupancy of the orbitals may not be the same, but at least for Ni(100) it has been shown that only the $d(xy)$ in-plane orbital is partially filled [28]. If the same holds for Cu(100)—Ni this may explain the lack of CO adsorption on this surface. The lack of surface states has also been invoked by Montano *et al.* [29] to explain the absence of CO adsorption on epitaxially grown Cu on Ni(100).

A second trend in the data concerns the capability of the surfaces to thermally dissociate or disproportionate CO. Only Ni is able to do so, the temperatures above which this process occurs being less than 400 K for Ni(110) [30], about 420 K for Ni(100) and more than 440 K and high CO

pressures for Ni(111). The reactivity of these surfaces is thus Ni(110) > Ni(100) > Ni(111), the same order as the roughness of the surfaces. This may be rationalised by the following arguments, where for simplicity a homonuclear diatomic is considered with potential energy function $V_{AB}(r_{AB})$, where r_{Ab} is the internuclear separation. For a diatomic to dissociate, the bond length must evidently increase, which leads to an increase in energy. Thus the effect of a nearby metal surface must be such that eventually the energy of the total system (metal plus diatomic) decreases upon stretching the diatomic bond. It is clear that the most likely situation for this to happen is one where the diatomic in its precursor state has its axis (roughly) parallel to the surface. Assuming pairwise additive potentials, *i.e.* that the diatomic–metal interaction can be written as the sum of the interactions of each atom with the metal, the total energy of the system is given by:

$$U_t = V_{AB}(r_{AB}) + V_{AB}(|R - \tfrac{1}{2}r_{AB}|) + V_{BM}(|R + \tfrac{1}{2}r_{AB}|) \quad (1)$$

where R is the center of mass coordinate of the diatomic molecule. The atom-surface potentials V_{AM} and V_{BM} have the same form for a homonuclear molecule and may be written

$$V_{AM}(\rho) = -E(z)\{1 + \beta \cos(2\pi\rho/a)\} \quad (2)$$

where z is the distance of the atom above the surface, a the periodicity of the lattice and β an amplitude factor. For a molecule with its axis parallel to the surface the total energy becomes:

$$U_t = V_{AB}(r_{AB}) - 2E(z) - 2\beta E(z) \cos(2\pi R/a) \cos(2\pi r_{AB}/a) \quad (3)$$

which is composed of three terms. The first term increases with r_{AB}, the second term is a constant for fixed distance above the surface and the third term may decrease with r_{AB} provided that $\cos(2\pi R/a) > 0$, *i.e.* that the center of mass position is favourable. The first and third terms of eqn. (3) are shown schematically in Fig. 9, together with their sum (— — —) and the activation energy for dissociation (E_{act}). The activation energy will be less if the (— · — ·) line (the atom surface potential) falls off more steeply with r_{AB}. This is determined by two factors, *viz.* $2\beta E(z)$, the amplitude of the potential around its mean value, and $\cos(2\pi R/a)$, the position of the center of mass.

In order to compare the three low-index faces, we note first that $\beta E(z)$ will be largest for the 'rough' (110) face and smallest for the 'smooth' (111) face. Of course, the center-of-mass position must be such that the atom surface potential actually decreases with r_{AB}, as is tacitly assumed in Fig. 9. However, this is a prerequisite for all three planes and thus largely irrelevant for statements about relative rates of dissociation. These are thus expected to increase in the order (111) < (100) < (110).

For a heteronuclear molecule the discussion given above will be slightly more involved, the terms V_{AM} and V_{BM} now being different, but qualitatively the same conclusions are expected to hold. The inability of copper to dissociate CO is then related to the low heat of adsorption of atomic carbon ($E(z)$ in eqn. (3)) whereas nickel, having a large binding energy for carbon

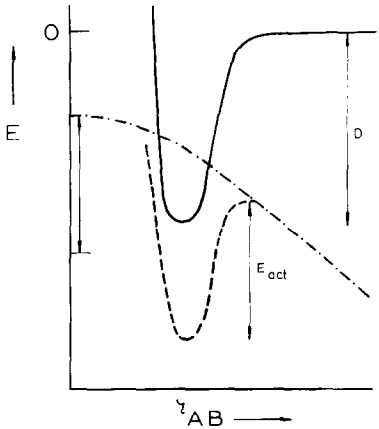

Fig. 9. Schematic diagram of the potential energy of a diatomic molecule as a function of interatomic distance r_{AB} (——), dissociation energy and activation energy for dissociation equal to D). (— · — ·) represents the interaction of the two atoms with the substrate as a function of r_{AB}. The amplitude of this cosine-like function is given by the unlabelled arrow and equal to $2\beta E(z)\cos(2\pi R/a)$ (*cf.* eqn. (3)). The sum of the two curves is given by (- - -) and leads to a lower activation energy for dissociation (E_{act}).

[31], is able to dissociate this molecule. It should be noted that the present picture for dissociation also predicts a larger tendency for steps and defects to dissociate adsorbates, since the local potential variations may be even larger than on a perfect crystal plane.

Acknowledgement

The investigations were supported by the Netherlands Foundation of Chemical Research (SON), with financial aid from the Netherlands Organisation for the Advancement of pure Research (ZWO).

References

1 G. Ertl and J. Küppers, *Low Energy Electrons and Surface Chemistry*, Verlag Chemie, Weinheim, 1974.
2 G. A. Somorjai, *Chemistry in Two Dimensions: Surfaces*, Cornell University Press, Ithaca, 1981.
3 M. Prutton, *Surface Physics*, Clarendon, Oxford, 1975.
4 R. M. A. Azzam and N. M. Bashara, *Ellipsometry and Polarised Light*, North Holland, Amsterdam, 1977.
5 R. H. Muller, *Adv. Electrom. Electrochem. Eng.*, *9* (1973) 167.
6 G. A. Bootsma and F. Meyer, *Surf. Sci.*, *14* (1969) 52.
7 G. A. Bootsma, L. J. Hanekamp and O. L. J. Gijzeman, in R. Vanselow and R. Howe (eds.), *Chemistry and Physics of Solid Surfaces IV*, Springer Series in Chemical Physics, Springer Verlag, Berlin, 1982, Vol. 20.
8 E. G. Keim, F. Labohm, O. L. J. Gijzeman, G. A. Bootsma and J. W. Geus, *Surf. Sci.*, *112* (1981) 52.

9 P. Hollins and J. Pritchard, *Surf. Sci., 89* (1979) 486.
10 J. Kessler and F. Thieme, *Surf. Sci., 67* (1977) 405.
11 K. Horn, M. Hussain and J. Pritchard, *Surf. Sci., 63* (1977) 244.
12 C. A. Pietersen, C. M. A. M. Mesters, F. H. P. M. Habraken, O. L. J. Gijzeman, J. W. Geus and G. A. Bootsma, *Surf. Sci., 107* (1981) 353.
13 C. M. A. M. Mesters, A. F. H. Wielers, O. L. J. Gijzeman, J. W. Geus and G. A. Bootsma, *Surf. Sci., 115* (1982) 237.
14 J. C. Campuzano, R. Dus and R. A. Greenler, *Surf. Sci., 102* (1981) 172.
15 O. L. J. Gijzeman, M. M. J. van Zandvoort, F. Labohm, J. A. Vliegenthart and G. Jongert, *J. Chem. Soc., Faraday II*, to be published.
16 K. Christmann, O. Schober and G. Ertl, *J. Chem. Phys., 60* (1974) 4719.
17 F. Labohm, C. W. R. Engelen, O. L. J. Gijzeman, J. W. Geus and G. A. Bootsma, *J. Chem. Soc., Faraday Trans. 1, 78* (1982) 2435.
18 J. C. Tracy, *J. Chem. Phys., 56* (1972) 2736.
19 H. H. Madden, J. Küppers and G. Ertl, *J. Chem. Phys., 58* (1973) 3401.
20 W. Erley and H. Wagner, *Surf. Sci., 74* (1978) 333.
21 T. J. Vink, M. M. J. van Zandvoort, O. L. J. Gijzeman and J. W. Geus, *Appl. Surf. Sci.*, to be published.
22 D. W. Goodman and M. Kiskinova, *Surf. Sci., 105* (1981) L265.
23 W. Erley and H. Wagner, *J. Catal., 53* (1978) 287.
24 C. M. A. M. Mesters, G. Wermer, O. L. J. Gijzeman and J. W. Geus, *Surf. Sci., 135* (1983) 396.
25 G. C. Bond, *Discuss. Faraday Soc., 41* (1966) 200.
26 W. H. Weinberg and R. P. Merrill, *J. Catal., 40* (1975) 268.
27 R. A. van Santen, *Recueil, 101* (1982) 121.
28 D. J. M. Fassaert and A. van der Avoird, *Surf. Sci., 55* (1972) 291.
29 P. A. Montano, P. P. Vaishnava and E. Boling, *Surf. Sci., 130* (1983) 191.
30 H. H. Madden and G. Ertl, *Surf. Sci., 35* (1973) 211.
31 J. M. Blakely, *Solid State Sci., 7* (1978) 333.